CWA 8:00 am–10:00 am

Rooms 314/315

Oxide-Confined VCSELs

Larry A. Coldren, *University of California–Santa Barbara, Presider*

CWA1 (Invited) 8:00 am

Oxide confinement: A revolution in VCSEL technology

D. G. Deppe, D. L. Huffaker, T.-H. Oh, *Microelectronics Research Center, Department of Electrical and Computer Engineering, The University of Texas at Austin, Austin, Texas 78712-1084*

In just three years since its first introduction,[1,2] the oxide-confined VCSEL has come to dominate much of the semiconductor laser research effort.[3–9] Its prominence in studies of semiconductor microcavity physics is expected to increase as well, as it represents a promising means of minimizing an optical mode volume. The ease of processing allows novel forms of two-dimensional arrays, and submicron feature sizes.

The oxide impact on low threshold VCSEL design can be two-fold. Its use as a dielectric aperture overcomes the lateral size Q limitation, and allows device scaling down to a few microns. Figure 1 shows a plot of threshold current versus aperture diameter for two different aperture designs differing in the oxide aperture thickness (labeled either $x = 1.0$ or $x = 0.97$) and placement within the cavity. The apertures are formed in VCSELs by use of half-wave cavity spacers and single InGaAs quantum well (QW) active regions, with a lower 26 pair AlAs/GaAs distributed Bragg reflectors (DBRs), and upper DBRs of six pairs of MgF/ZnSe. For both types the threshold current continues to decrease with decreasing aperture size down to ~2 μm diameter, with a minimum of threshold of ~60 μA. For sizes smaller than 2 μm diameter various loss mechanisms lead to sharp increase in threshold. Although the two aperture designs show similar threshold characteristics, the optical modes are found to be quite different for the sub-2 μm device sizes.[9]

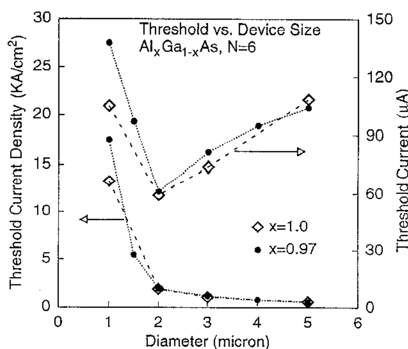

CWA1 Fig. 1 Plot of threshold current and current density as a function of aperture size for a VCSEL with a 26-pair AlAs/GaAs lower DBR.

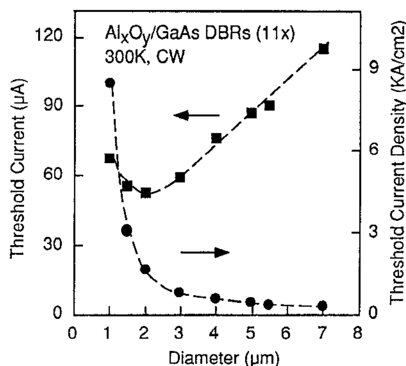

CWA1 Fig. 2 Plot of threshold current and threshold current density as a function of aperture size for a VCSEL with an 11-pair Al_xO_y/GaAs lower DBR.

The second impact of the oxide is in forming high contrast Al_xO_y/GaAs DBRs that can be monolithically integrated beneath the VCSEL cavity.[8] The shortening of the effective cavity length allows lateral size reduction smaller than what can be achieved with AlAs/GaAs DBRs. Figure 2 shows a plot of threshold current versus aperture size for a novel VCSEL design that uses an 11-pair Al_xO_y/GaAs DBR, again with a half-wave cavity spacer and a single InGaAs QW active region. Although the minimum threshold current is again achieved for ~2 μm aperture diameter, the threshold increase for smaller sizes is more gradual than in Fig. 2. We believe that with optimization of the high contrast DBR and gain region, good threshold scaling might be achieved down to sub 1 μm diameters.

This work is supported by the AFOSR under contract No. F49620-96-1-0336, the DARPA funded Center for Optoelectronic Science and Technology, and the Texas Advanced Technology Program under TP-210.

1. D. L. Huffaker, D. G. Deppe, K. Kumar, T. J. Rogers, Appl. Phys. Lett. **65**, 97 (1994).
2. D. L. Huffaker, J. Shin, D. G. Deppe, Electron. Lett. **30**, 1946 (1994).
3. K. D. Choquette, R. P. Schneider, Jr., K. L. Lear, K. M. Geib, Electron. Lett. **30**, 2043 (1994).
4. K. L. Lear, K. D. Choquette, R. P. Schneider, Jr., S. P. Kilcoyne, Appl. Phys. Lett. **66**, 2616 (1995).
5. G. M. Yang, M. H. MacDougal, P. D. Dapkus, Electron. Lett. **31**, 886 (1995).
6. M. J. Ries, T. A. Richard, S. A. Maranowski, N. Holonyak, Jr., E. I. Chen, Appl. Phys. Lett. **65**, 740 (1994).
7. M. H. MacDougal, G. M. Yang, A. E. Bond, C.-K. Lin, D. Tishinin, P. D. Dapkus, IEEE Photon. Technol. Lett. **8**, 310 (1996).
8. T.-H. Oh, D. L. Huffaker, D. G. Deppe, Appl. Phys. Lett. **69**, (Nov. 18, 1996).

CWA2 8:30 am

Small and large signal modulation of 850 nm oxide-confined vertical-cavity surface-emitting lasers

K. L. Lear, V. M. Hietala, H. Q. Hou, J. Banas, B. E. Hammons, J. Zolper, S. P. Kilcoyne, *Sandia National Laboratories, MS 0603/PO Box 5800 / Albuquerque, New Mexico 87185-0603; E-mail: kllear@sandia.gov*

We have previously demonstrated record modulation bandwidths for oxide-confined vertical-cavity surface-emitting lasers (VCSELs) based on strained InGaAs/GaAs quantum wells.[1] The monolithic oxide-confined structure[2] provides good optical confinement, low thresholds, efficient operation, and acceptable thermal resistance; these qualities promote high speed operation. Here we report work on nominally 850 nm wavelength oxide-confined VCSELs with modulation bandwidths in excess of 20 GHz.

High modulation bandwidths were achieved with an oxide confined VCSEL structure modified to decrease parasitic circuit elements. Figure 1 shows a schematic cross section of the VCSEL with a corresponding small signal equivalent circuit. Coplanar waveguide pads designed for on wafer probing were placed on a 5-μm-thick polyimide to reduce the capacitance between the pad and the conducting substrate to approximately 50 fF. The device capacitance was further reduced by implanting the mesa area lying outside the active region where thin oxide layers would otherwise result in high capacitance.

The laser diodes feature DC characteristics that are important for high speed modulation. Figure 2 shows quasi-static light-current and voltage-current characteristics indicating a submilliampere threshold current, operation to several times threshold before thermal rollover, good efficiency coupled into the fiber, and moderate resistance for this size of device (~4 × 4 μm²). This device also operated in the fundamental mode to approximately 4 mA as necessary to obtain increasing photon densities in the mode. Other similar sized devices remained single moded at all operating currents.

The small signal response of VCSELs as a function of bias current was measured with use of a calibrated vector network analyzer with on wafer probing and a 30 GHz photodetector connected through approximately 2 m of the multimode fiber. The modulation response at various bias currents was fit with a traditional damped resonator model to extract the reso-

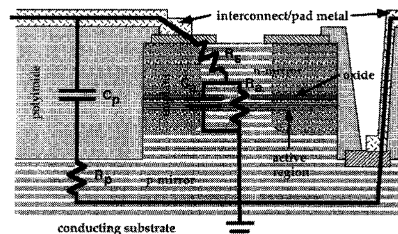

CWA2 Fig. 1 Schematic cross section of high-speed VCSEL structure with superposed equivalent circuit.

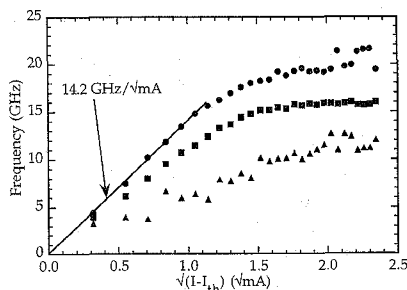

CWA2 Fig. 2 Resonance frequency (squares), -3 dB frequency (circles), and equivalent damping frequency ($\gamma/2\pi$) (triangles) as a function of square root of current above threshold.

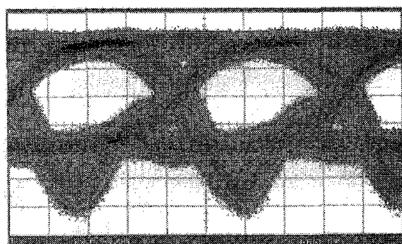

CWA2 Fig. 3 Eye diagram generated by 12 Gb/s digital modulation of multimode VCSEL linked to a photodetector and inverting amplifier without filtering.

nant frequency and equivalent damping frequency ($\gamma/2\pi$). These quantities for a $\sim 4 \times 4$ μm^2 laser with 0.5 mA threshold current are plotted in Fig. 2 along with the -3 dB bandwidth. At low bias currents, the bandwidth and resonant frequency increase in proportion to the square root of the current above threshold as expected from the conventional rate equation analysis. The rate of increase in this region yields a modulation current efficiency factor (MCEF) of 14.2 GHz/$\sqrt{}$mA, which is slightly lower than the highest value we previously reported for oxide-confined VCSELs with InGaAs quantum wells.[1] The resonant frequency increases steadily to 15 GHz at 2.7 mA and then becomes nearly constant. The -3 dB bandwidth is as high as 21.5 GHz.

Large signal, digital modulation experiments were also performed. Figure 3 shows the eye diagram during a 12 Gb/s test that uses $\sim 8 \times 8$ μm^2 multimode lasers with both levels above threshold. Bit error rates as low as 10^{-13} were observed in preliminary investigations at this data rate. Reducing the "0" level slightly below threshold resulted in substantial, pattern dependent jitter. Jitter measurements will be presented.

This work was supported by the United States Department of Energy under Contract DE-AC04-94AL85000.

1. K. L. Lear *et al.*, Electron. Lett. **32**(5), 457 (1996).
2. K. D. Choquette *et al.*, Photon. Technol. Lett., 7(11), 1237 (1995).

CWA3 8:45 am

Novel intracavity modulator integrated with a vertical-cavity surface-emitting laser

S. F. Lim, L. P. Chen, G. S. Li, W. Yuen, K. Y. Lau, C. J. Chang-Hasnain, *Department of Electrical Engineering and Computer Sciences, 211-196 Cory Hall, University of California, Berkeley, California 94720*

As vertical-cavity surface-emitting lasers (VCSELs) become more prominent in many applications, the need arises to be able to modulate these lasers to high frequencies. Although fairly large bandwidths have been attained with direct current modulation, the inevitable frequency chirping and intrinsic parasitics associated with carrier density variations imposes limits on both digital and large-signal AM applications. In this work we demonstrate a novel modulation technique for a VCSEL in which the drive signal is applied to the voltage across a quantum well absorber, which is embedded in the VCSEL mirror stack. As a result, the mirror reflectivity changes, and hence the laser output power is modulated. This technique is expected to be very high speed with low chirp and high modulation efficiency. Here, we show preliminary experimental results of such a novel laser, which indicate a -3 dB bandwidth of $\sim$3 GHz, limited only by the resonant frequency of an unoptimized VCSEL structure.

Figure 1 shows a schematic of the top-emitting device structure. It is comprised of n-doped distributed Bragg reflector (DBR) pairs on a GaAs substrate, followed by a 1-λ spacer that contains two 80-Å $In_{0.2}Ga_{0.8}As$ quantum wells as the active region, a p-doped DBR stack that contains a $3\lambda/4$-thick AlAs oxidation layer for current confinement, a $5\lambda/4$ spacer with one 80-Å $In_{0.2}Ga_{0.8}As$ quantum well as the absorber, and n-doped DBR pairs. The tested devices had approximately 26-μm diameter oxide-defined apertures. The p-contact is used to forward bias the active region while the top n-contact is used to control the voltage across the quantum well absorber. This quantum well modulator is placed at an optical intensity peak within the DBR stack, resulting in high impact on the device output for a small modulating voltage. Also, because VCSELs are very sensitive to their mirror reflectivities, the presence of the modulator within the mirror stack renders the modulator highly efficient.

Figure 2 shows the output power-current (L-I) curve characteristic of these devices for different reverse bias voltages across the absorber. Peak output power is typically more than 1 mW, and the threshold current is approximately 7 mA.

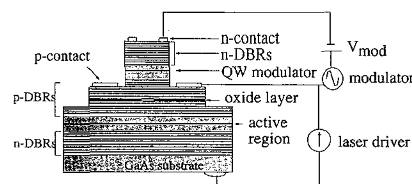

CWA3 Fig. 1 Schematic of the structure.

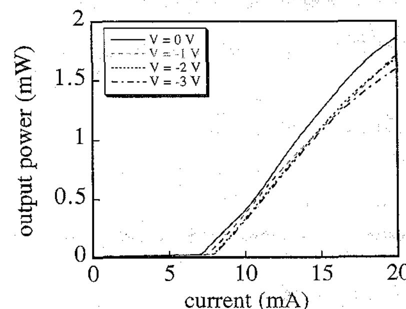

CWA3 Fig. 2 Power-current (L-I) curve for a typical device under different modulator dc biases.

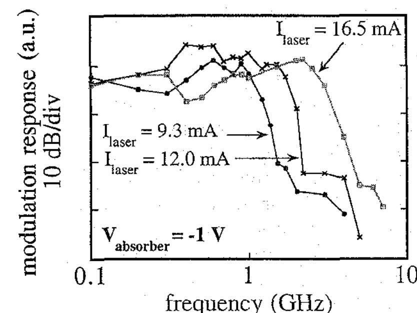

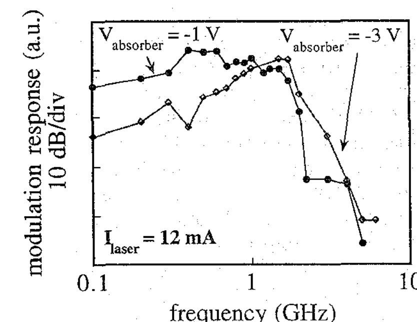

CWA3 Fig. 3 (a) Modulation response for different laser drive currents at a fixed (-1 V) modulator bias (b) Modulation response for different modulator biases at a fixed laser drive current (12 mA).

The frequency response is shown in Figs. 3a and 3b for different laser bias currents and different reverse bias voltages across the absorber, respectively. Figure 3a shows increase in the bandwidth as the laser current is increased while the modulator dc bias is kept constant at -1 V. At $I_{laser} = 9.3$ mA, the -3 dB point is at 1.1 GHz. Increasing I_{laser} to 16.5 mA broadens the bandwidth to 3.2 GHz. In Fig. 3b, I_{laser} is kept constant at 12 mA. Application of -1 V across the absorber produced 1.7 GHz bandwidth whereas increasing the modulator reverse bias to -3 V produced 2.7 GHz bandwidth. These trends indicate that with a structure optimized for higher resonant frequency,